DOI 10.31489/2022PH3/52-60

UDC 678.742.3(54.03)

Q.N. Berdinazarov*, E.O. Khakberdiev, N.F. Normurodov, N.R. Ashurov

Uzbekistan Academy of Sciences, Institute of Polymer Chemistry and Physics, Tashkent, Uzbekistan
*(*E-mail: qodirberdinazarov@mail.ru)*

Mechanical and thermal degradation properties of Isotactic Polypropylene Composites with Cloisite15A and Cloisite20A

This work studies the influence of maleic anhydride grafted polypropylene (PP-g-MA) content on thermal and mechanical properties of polypropylene (PP) composites with two types of clays, differing modifier density in the interlayer space, Cloisite15A and Cloisite20A. PP/clay composites are melt blended in presence of different content of PP-g-MA from 3, 6, 9, and 12 wt.%. It is found that Cloisite15A with a high density of the modifier promotes the formation of intercalated structures, while Cloisite20A with a low density of the modifier, predominantly exfoliated nanocomposites are formed. In the first case, the structure tends to become intercalated whilst composites with Cloisite20A favor the formation of predominantly exfoliated structures. The formation of the nanocomposite is accompanied by a significant increase in thermal stability (50% weight loss is observed at temperatures of 360°C and 430°C for polypropylene and nanocomposites based on it, respectively). An analysis of the mechanical properties of nanocomposites generally indicates an increase in the elastic modulus by 15-20%, and this effect is more pronounced for exfoliated structures, the yield strength practically does not change and the elongation at break decreases noticeably.

Keywords: polypropylene, clay, composite, polypropylene grafted maleic anhydride, intercalation, exfoliation, oxidation, montmorillonite.

Introduction

Recently conducted researches in polymer science have shown finer dispersed inorganic layered silicates or smectite clays through the organic polymer, increasing its mechanical, thermal, barrier, and fire retardant properties [1–7]. Layered silicates are made up of several hundred thin platelets stacked in orderly particles or tactoids with dimensions of 8–10 μm. Each disk-shaped platelet has a large aspect ratio of approximately 100–1000 and is easily agglomerated due to the interlayer van der Waals forces. Accordingly, clay particles should be homogeneously finer dispersed and exfoliated as individual platelets within the polymer matrices to accomplish the ultimate properties. Moreover, the lower clay content is also essential to achieve the large contact surface area between the polymer matrix and the fillers and to obtain good dispersion by alleviating the clay aggregation [8, 9].

Thermal stability of PP/clay composites was considerably increased as soon as obtained exfoliated structure [10–16]. The authors concluded that the improvement in the thermal properties was correlated with lower oxygen permeability resulting from an increased diffusion path for oxygen as well as volatile decomposition products. PP-g-MA was found the most effective compatibilizer for PP/clay composites in many articles [17–20]. There are a lot of publications that investigate the effect of different clay modification techniques [21, 22].

Phase diagram of polymer – clay mixture, proposed by Ginzburg et al., revealed that increased length and density of grafted chains led to improved miscibility of the clay and the polymer, in its turn, proper miscibility contributes to exfoliated structure in the wide range of clay volume ratio. In the case of short surfactant macromolecules, the polymer is not likely to insert space between the clay layers. This causes immiscible equilibrium morphology for major values of the Flory – Huggins parameter and the clay volume ratio. There is also a limitation to strong interaction between grafted chains and polymer macromolecules [23].

For different surfactant lengths, surfactant coverage and surfactant – matrix enthalpic, Balazs et al. studied morphological behavior of polymer clay composites by employing their model named self-consistent field calculation. According to their model, it turned out that a longer organic modifier provides better intercalation of polymer macromolecules to penetrate the space between clay platelets. But, the density of surfactant should be reasonable because dense coverage makes intercalation and/or exfoliation impossible [24].

Accordingly, in this paper isotactic PP, PP-g-MA, and two types of clays were chosen in obtaining composites. This study aims to explore the properties of PP/clay nanocomposites obtained with different modifier densities between interlayer spaces in the variation of compatibilizer content.

Experimental:

Materials: Isotactic PP (J-170T) with MFI = (2.16 kg, 230ºC) 21 g/10 min was kindly provided by JV Uz-Kor Gas Chemical LLC. PPMA with 2,5 wt.% maleic anhydride content and MFI = (2,16 kg, 230 ºC) >200 g/min was provided by JV UzAuto CEPLA LLC as a gift. Cloisite15A, (spacing d_{001}=2,96 nm, dimethyl dehydrogenated tallow ammonium conc. 1,25 meq/g), Cloisite20A, (spacing d_{001}=2,47 nm, dimethyl dehydrogenated tallow ammonium conc. 0,95 meq/g) Southern Clay Products, Inc., Gonzales, TX.

Preparation: Components melt blended in Brabender Plastograph (Germany). First PP and PPMA were introduced into plastograph after getting molten mass clay was introduced and kept for 8 min 150 rpm to provide better mixing components one another. Next, tensile test samples were prepared by injection-molding machine Mercator 1971 (Poland). The name of samples and their content ratios are given in Table 1.

Table 1

Name of the obtained samples and their contents

Name of samples	PP, %	PP-g-MA, %	Cloisite15A, %	Cloisite20A,%
PP	100	-	-	-
PPMA	-	100	-	-
PP/MA10	90	10	-	-
PP/MA20	80	20	-	-
15A3	94	3	3	-
15A6	91	6	3	-
15A9	88	9	3	-
15A12	85	12	3	-
20A3	94	3	-	3
20A6	91	6	-	3
20A9	88	9	-	3
20A12	85	12	-	3

XRD measurements

XRD measurements were conducted with Rigaku Miniflex 600 (Japan) in the condition of 40 kV voltage, 15 mA current and 0.02° step.

DSC and TGA measurements

Thermal properties of the samples studied by DSC and TGA analysis were conducted simultaneously, in the range from room temperature to 600ºC by Linseis thermal analysis PT1610.

Mechanical analysis

Tensile tests were conducted according to ASTMD 638 in Shimadzu AG-X PLUS (Japan). For measuring tensile module (E), 1 mm/min crosshead speed was chosen until 0,3% deformation, after that crosshead speed increased immediately to 20 mm/min for further exploring yield stress ($\boldsymbol{\sigma}$) and deformation ($\boldsymbol{\varepsilon}$).

MFI measurement

MFI was measured according to ASTMD 1238 using a Zwick extrusion plastometer (Germany) at 230 ºC/2,16 kg.

Results and Discussion

Small angle X-ray diffraction

Small angle X-ray (SAXS) diffraction is identical for characterizing clay dispersion in the polymer matrix [25–27]. The basal spacing of the silicate layer (d001) was calculated with Bragg's law: $n\lambda=2d\sin\theta$. Figures 1 and 2 show the SAXS pattern of obtained samples. The difference between these two organically modified clays is modifier volume and interlayer distance d (which Cloisite15A has greater than Cloisite20A) [28]. Cloisites have two main peaks, the second peak at $2\theta=7{,}2°$ (d001=1,2 nm) corresponding to interlayer distance of pure unmodified montmorillonite (MMT), the first peak occurs in $2\theta=2{,}88°$ in Cloisite15A corresponding to intercalation of MMT as a result of modifier penetration during modification while in Cloisite20A, this peak accounts for in $2\theta=3{,}68°$. SAXS curves in Figures 1 and 2, compare the effect of PP-g-MA content on the intercalation degree of Cloisite15A and Cloisite20A. There was a considerable difference between the dispersion of clay through the PP matrix. While composites with Cloisite15A show an intercalated structure, Cloisite20A achieves exfoliation except for 20A3. In the case of Cloisite15A,

the first peak in 2θ=2,8° shifts towards small angles about 2θ=2,3° corresponding to d=38,25Å, however, 15A9 has slightly smaller angles than others, indicating all samples' intercalation. The second peak also decreased from 2θ=7,2° to 2θ=4,7°. With respect to the intensity of the peaks, the smallest intensity was seen in both main peaks in 15A9. This reduction in the peak intensity can be interpreted as the formation particular amount of exfoliated structure as well as intercalated. When it comes to Cloisite20A, except for composite with 20A3 all had a considerable shift in peaks to lower than 2θ=2° angle, as a result of exfoliation. The reason for exception 20A3 is the lack of compatibilizer to achieve finer dispersion of clay in the polymer matrix. The occurrence of exfoliation in the composites with Cloisite20A can be proved to shift the first peak smaller angle in relation to pure Cloisite20A.

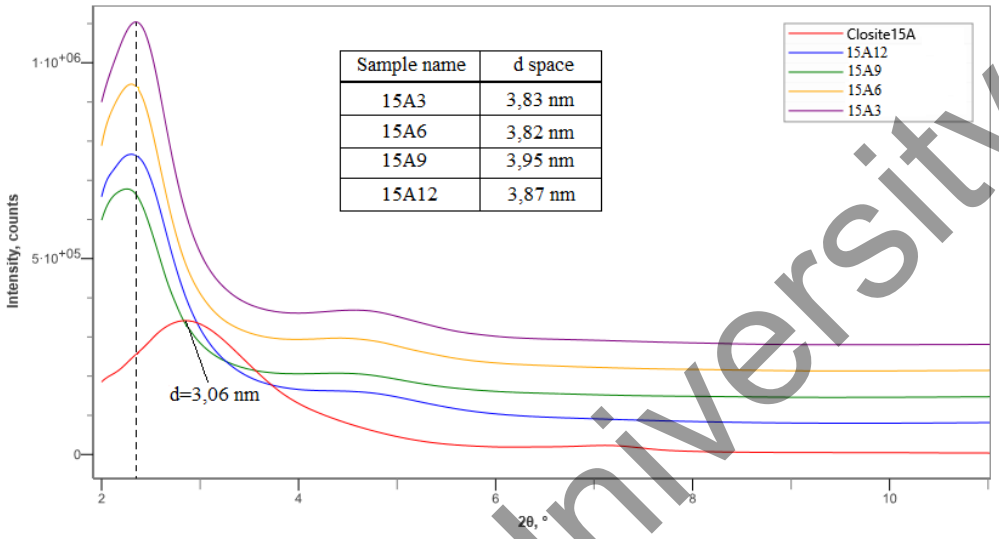

Figure 1. PP and Cloisite15A composites small angle X-ray curves

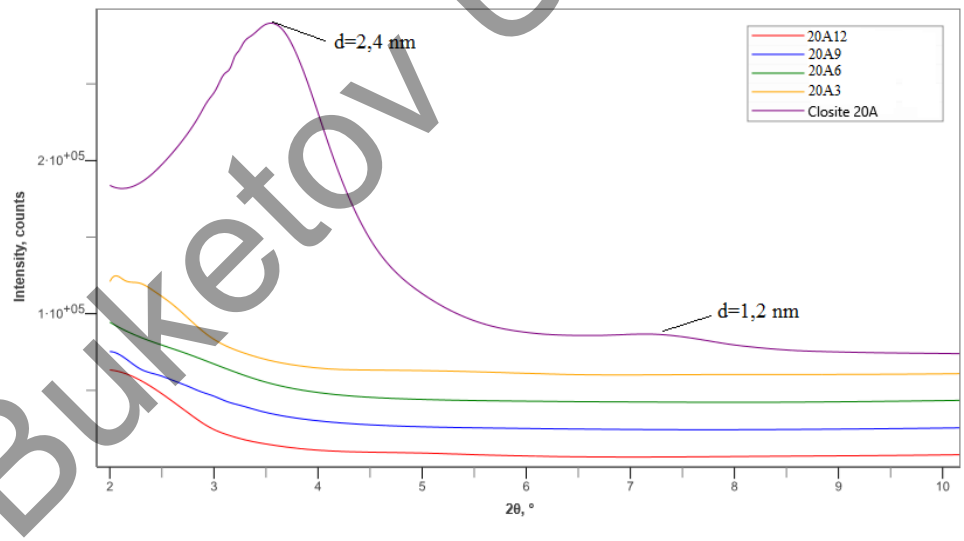

Figure 2. PP and Cloisite20A composites small angle X-ray curves *MFI*

Figure 3 compares MFIs of PP and PP-g-MA blends. PP-g-MA shows more than 200 g/10 min MFI while PP has 21 g/10 min. The presence of 10 wt. % PP-g-MA in PP/PPMA blends MFI accounts for 56 g/10 min and further addition of PP-g-MA increases MFI to 94 g/10 min. This is due to the low molecular weight of PP-g-MA and, as shown in a number of works [14, 15, 23, 24], it is oligomeric functionalized PP that provides favorable conditions for intercalation in the interlayer space and subsequent exfoliation of MMT particles. For PP and clay systems, MFI decreases as soon as the formation of exfoliated and intercalated structures. Our compositions also exhibited such kind of manner (Figure 4). For composites with Cloisite15A, when the ratio of compatibilizer/filler was 1, MFI is 58,6 g/10 min and as compatibilizer content increases MFI decreases to 17,5 g/10 min in the 15A9, however, subsequent addition of PP-g-MA caus-

es slight growth in the 15A12. The initial reduction in MFI is related to the extension of clay particle dimensions as a result of intercalation. When PP-g-MA content reaches saturation point, that is 9 wt.%, additional PP-g-MA causes to increase in MFI. With regard to composites with Cloisite20A, an optimal amount of compatibilizer is 6 wt.% and extra compatibilizer by not taking part in intercalation or exfoliation just leads to the increase in the melt flow. Intercalated centers in the form of physical knots (similar to crosslinking), as PP-g-MA increases, leads to an increase in the viscosity of the composition, for exfoliated structures (uniform distribution of nanoparticles) an extreme viscosity dependence is observed with a minimum at a PP-g-MA content of 6% wt. For these structures, the contribution of low-viscosity PP-g-MA above 6 wt.% becomes noticeable.

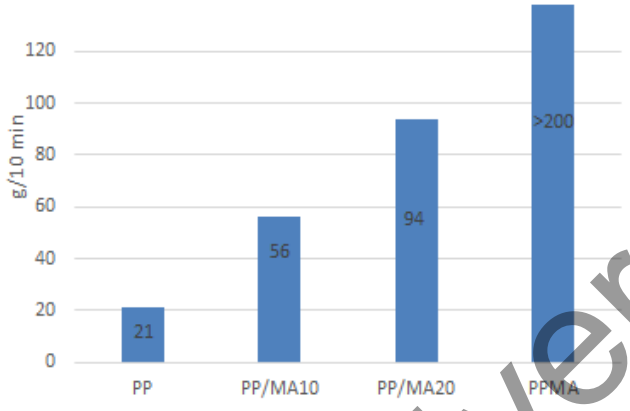

Figure 3. MFI of PP and PP-g-MA blends

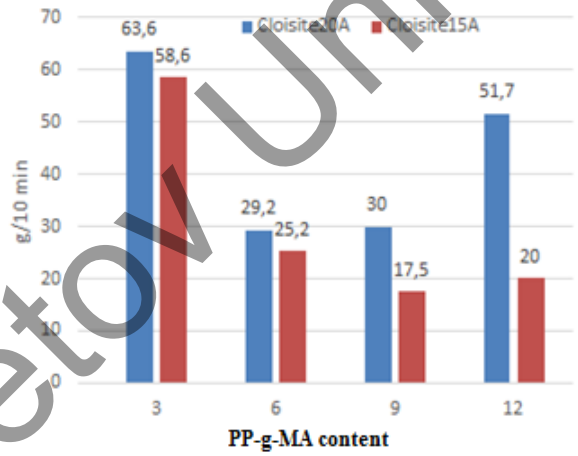

Figure 4. MFI of composites based on Cloisite15A and Cloisite20A.

DSC and TGA measurements

DSC curves for PP and PPMA blends show different oxidation behavior while the melting temperature of the samples is almost the same. Showing a melting point of 158,5°C, PP stands stable until 220°C, and subsequent heating causes intensive oxidation. PP-g-MA with a melting point of 160,6°C, is immediately engaged in oxidation after melting. Their blends indicate thermal behavior corresponding to individual components. As PP-g-MA content increases in the blend, oxidation occurs at relatively lower temperatures (Figure 5). Figure 6 compares DSC curves of composites with Cloisite15A, reflecting differences only in oxidation behavior. In composites with 9 and 12 wt.%, although PPMA leads to oxidation due to intercalation, engaging in oxidation is reduced. DSC curves of composites with Cloisite20A show distinction in both melting point and oxidation (Figure 7). 20A3, intercalated composite, has a melting point of 159,1ºC and gets involved in oxidation intensively after melting. However, when PP-g-MA content is increased by 6 wt.% the composite is stable to oxidation until 188 ºC. Due to the penetration of PP-g-MA molecules into the interlayer space of filler, this exfoliated composite has a lower melting point temperature, which is 157,9 ºC, in this case. Even though there is exfoliation, the subsequent addition of PP-g-MA again causes more sensitive oxidation behavior and increased melting points, in the compositions with 9 and 12 wt.% of Cloisite20A.

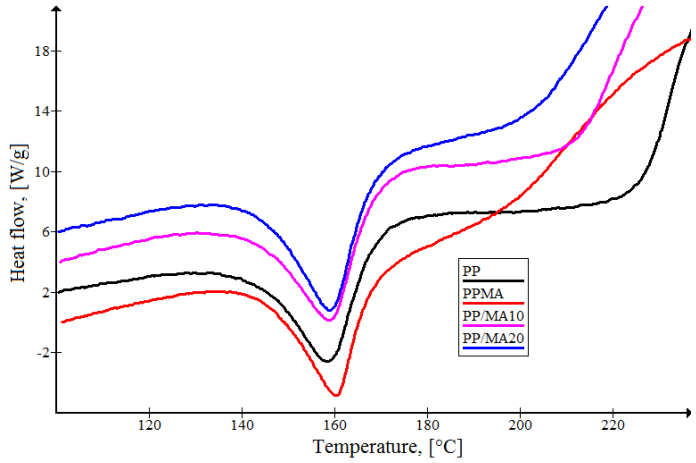

Figure 5. DSC curves of PP and PP-g-MA blends

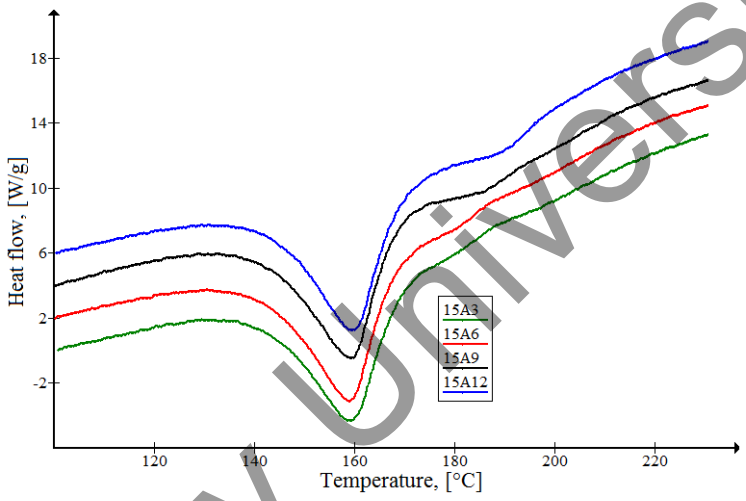

Figure 6. DSC curves of composites with Cloisite15A.

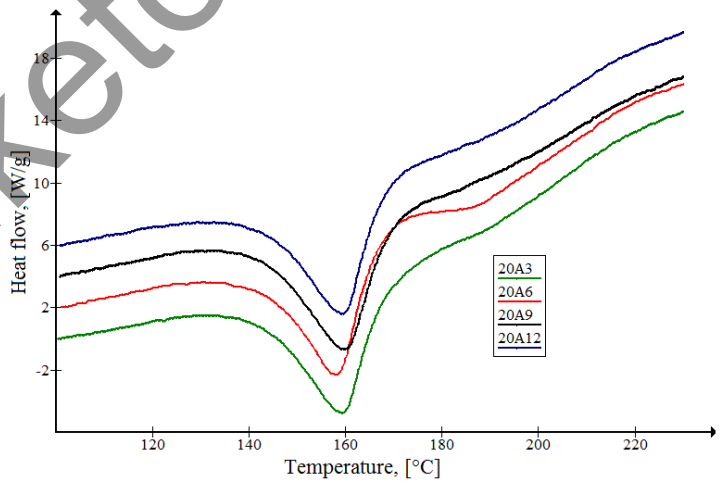

Figure 7. DSC curves of composites with Cloisite20A

Except for DSC, TGA analyses of obtained samples also were conducted, too. In Figure 8, PP starts mass loss at 237ºC (onset temperature of degradation) while in the case of PP-g-MA accounts for 256ºC. Furthermore, after starting degradation, PP engages in degradation more intensively than PP-g-MA. PP and PP-g-MA blends show different degradation mechanisms, as increases PP-g-MA content in the blends degradation curve of the blend tends to become similar to PP-g-MA. However, PP/MA10 and PP/MA20

blends start degradation at lower temperatures relative to PP. The onset temperature of degradation must have been between the degradation temperatures of PP and PP-g-MA according to the rule of polymer additiveness. The reason for this is that PP-g-MA makes PP sensitive toward oxidation, due to its thermal behavior, during melt processing components, according to the DSC curves in Figure 5. PP-g-MA uptakes oxygen during melt processing and then this absorbed oxygen leads to degradation by generating free radicals which cause PP/MA10 and PP/MA20 blends mass loss in relatively earlier temperatures [9]. With regard to TGA analysis of composites obtained with Cloisite15A and Cloisite20A, though PP shows superior thermal stability to oxidation among samples in DSC analysis, thermal degradation properties – mass loss – of PP are inferior to that of PP/clay nanocomposites (Figure 9). In PP/clay nanocomposites, clay acts as an excellent insulating barrier that slows the release of gas from decomposition, so the degradation temperature increases. In general, the presence of clay in the PP tends to the increased thermal stability of the polymer [29].

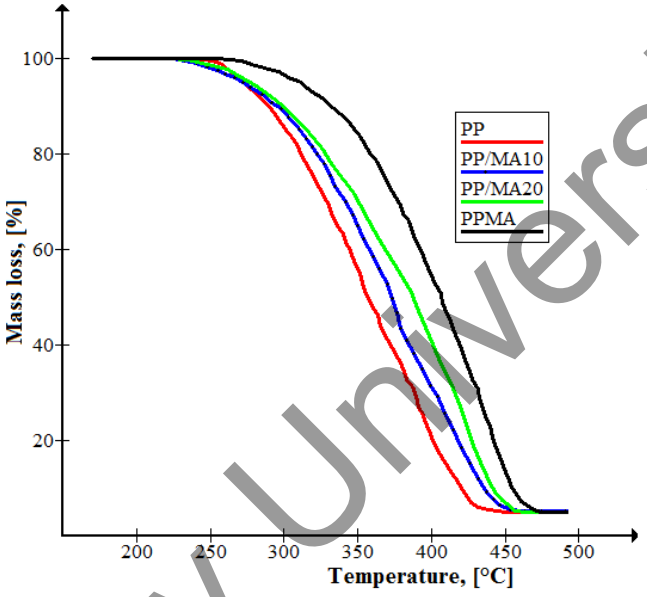

Figure 8. TGA of PP and PPMA blends

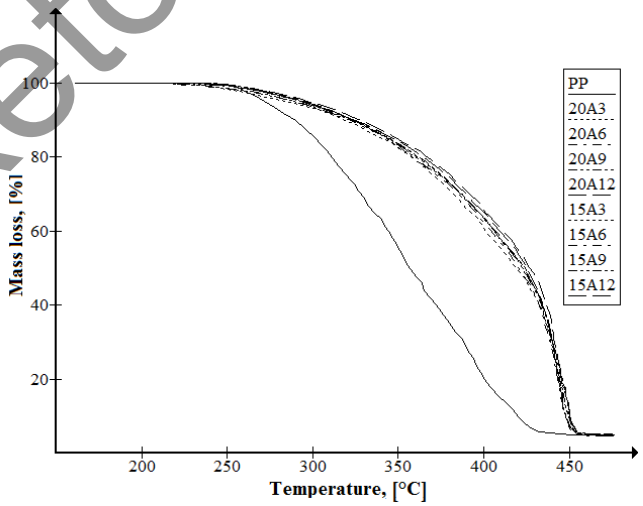

Figure 9. TGA of PP and PP/clay composites

Mechanical measurements

Table 2 presents tensile properties – tensile module (**E**), yield stress (**σ**), and elongation at break (**ε**). The neat PP itself possesses superior mechanical with the best **E** and **σ**, while PPMA has good **ε** which is approximately five times more than neat PP. The addition of PP-g-MA to PP makes PP tougher that **ε** in-

creases and reduces **E** and **σ** PP tends to become more brittle. In the compositions with Cloisite15A, as PP-g-MA increases, unlike PP/PP-g-MA blend, **E** and **σ** also increase; filler content is constant. The reason for this behavior is the development of nano-dispersed clay particles through the matrix as can be seen from SAXS, shifting of the peak in d_{001} to small angles. In the case of composites with Cloisite20A, a saturation of composite with PP-g-MA occurs when PP-g-MA content is 6 wt.% and further addition of compatibilizer leads mechanical properties to diminish by causing oxidation of composite in high temperature.

Table 2

Mechanical properties of obtained PP/clay composites.

Sample names	E, [MPa]	**σ**, [MPa]	**ε**, [%]
PP	922±68	36,2±1,2	845±90
PP/MA10	918±54	36,5±1,2	738±93
PP/MA20	770±7	29,9±0,7	984±150
PPMA	713±61	26,2±1,6	697±52
15A3	946±61	32,8±0,6	18,5±2
15A6	960±52	34,5±1,2	17,8±3,8
15A9	968±49	35,2±0,8	127±18
15A12	1008±41	35,3±1,1	102±29
20A3	1000±51	35,4±0,8	12,7±2
20A6	1087±19	37,6±0,3	52±7
20A9	1002±52	35,9±0,5	17,3±5
20A12	932±51	35,4±0,4	16,8±3

Conclusions

Studies were carried out on the formation of nanocomposites of isotactic polypropylene with modified MMT (Cloisite15A, Cloisite20A), differing modifier densities in the interlayer space. To ensure the diffusion of PP into clays, PP-g-MA (2.5 wt.%) was employed as a compatibilizer, the amount of which is a mixture with PP-g-MA varied within 3, 6, 9, and 12 wt.%. It was found that MMT with a high density of the modifier (Cloisite15A) promotes the formation of intercalated structures, while MMT with a low density of the modifier (Cloisite20A), predominantly exfoliated nanocomposites are formed. In the first case, an increase in the content of PP-g-MA leads to an expansion of the interlayer space (from 30.6 to 39.5 Å). In composites with Cloisite20A, only 3 wt.% content of PP-g-MA shows the formation of mixed intercalated and exfoliated structures, while subsequent increasing compatibilizer content favors the formation of predominantly exfoliated structures. The observed structures are reflected in the viscosity parameter, nanocomposites intercalated with an increase in less viscous PPMA due to limitations associated with the intercalation of macromolecules in the interlayer space and the presence of a specific interaction with the modifier and the clay surface increase markedly (from 65 to 20 g/min), whereas the exfoliation of the structure passes through a minimum in the region between 6 and 9% by weight of PPMA. The formation of the nanocomposite is accompanied by a significant increase in thermal stability (50% weight loss is observed at temperatures of 360°C and 430°C for polypropylene and nanocomposites based on it, respectively). An analysis of the mechanical properties of nanocomposites generally indicates an increase in the elastic modulus by 15–20% (considering the presence of low-modulus PP-g-MA), and this effect is more pronounced for exfoliated structures, the yield strength practically does not change, and the elongation at break decreases significanly. From a practical point of view, heat-resistance properties of intercalated and exfoliated nanocomposites (with a content of 9–12 wt.% and 6 wt.% PP-g-MA, respectively) with enhanced characteristics according to the tensile module and moderate deformability (more than 100%) is interesting.

Acknowledgements

The authors of this work acknowledge JV Uz-Kor Gas Chemical LLC for kindly providing PP grades. For supplying with PP-g-MA JV, UzAuto CEPLA LLC is gratefully acknowledged.

References

1 Gabr, M. H., Okumura, W., Ueda, H., Kuriyama, W., Uzawa, K., & Kimpara, I. (2015). Mechanical and thermal properties of carbon fiber/polypropylene composite filled with nano-clay. *Composites Part B: Engineering, 69*, 94–100. https://doi.org/10.1016/j.compositesb.2014.09.033

2 Dolgov, V.V., Ashurov, N.R., Sheveleva, E.E., & Khakberdiev, E.O. (2013). Strength-strain, barrier, thermal, and fire-resistance properties of nanocomposites based on linear polyethylene with montmorillonite. *Russian Journal of Applied Chemistry, 86*(12), 1885–1896. https://doi.org/10.1134/S1070427213120148

3 Villaluenga, J. P. G., Khayet, M., López-Manchado, M. A., Valentin, J. L., Seoane, B., & Mengual, J. I. (2007). Gas transport properties of polypropylene/clay composite membranes. *European polymer journal, 43*(4), 1132-1143. https://doi.org/10.1016/j.eurpolymj.2007.01.018

4 Kanny, K., Jawahar, P., & Moodley, V. K. (2008). Mechanical and tribological behavior of clay–polypropylene nanocomposites. *Journal of materials science, 43*(22), 7230-7238. https://doi.org/10.1007/s10853-008-2938-x

5 Lee, S. Y., Kang, I. A., Doh, G. H., Kim, W. J., Kim, J. S., Yoon, H. G., & Wu, Q. (2008). Thermal, mechanical and morphological properties of polypropylene/clay/wood flour nanocomposites. *Express Polymer Letters, 2*(2), 78-87. 10.3144/expresspolymlett.2008.11

6 Zhao, C., Qin, H., Gong, F., Feng, M., Zhang, S., & Yang, M. (2005). Mechanical, thermal and flammability properties of polyethylene/clay nanocomposites. *Polymer Degradation and Stability, 87*(1), 183-189. https://doi.org/10.1016/j.polymdegradstab.2004.08.005

7 Kato, M., Usuki, A., Hasegawa, N., Okamoto, H., & Kawasumi, M. (2011). Development and applications of polyolefin–and rubber–clay nanocomposites. *Polymer journal, 43*(7), 583-593. https://doi.org/10.1038/pj.2011.44

8 Hotta, S., & Paul, D. R. (2004). Nanocomposites formed from linear low density polyethylene and organoclays. *Polymer, 45*(22), 7639-7654. https://doi.org/10.1016/j.polymer.2004.08.059

9 Zdiri, K., Elamri, A., & Hamdaoui, M. (2017). Advances in thermal and mechanical behaviors of PP/clay nanocomposites. *Polymer-plastics technology and engineering, 56*(8), 824-840. https://doi.org/10.1080/03602559.2016.1233282

10 Bertini, F., Canetti, M., Audisio, G., Costa, G., & Falqui, L. (2006). Characterization and thermal degradation of polypropylene–montmorillonite nanocomposites. *Polymer degradation and stability, 91*(3), 600-605. https://doi.org/10.1016/j.polymdegradstab.2005.02.027

11 Liu, X., Wu, Q., Berglund, L. A., Lindberg, H., Fan, J., & Qi, Z. (2003). Polyamide 6/clay nanocomposites using a cointercalation organophilic clay via melt compounding. *Journal of applied polymer science, 88*(4), 953-958. https://doi.org/10.1002/app.12031

12 Xie, S., Zhang, S., Wang, F., Liu, H., & Yang, M. (2005). Influence of annealing treatment on the heat distortion temperature of nylon-6/montmorillonite nanocomposites. *Polymer Engineering & Science, 45*(9), 1247-1253. https://doi.org/10.1002/pen.20359

13 Tang, Y., Hu, Y., Song, L., Zong, R., Gui, Z., Chen, Z., & Fan, W. (2003). Preparation and thermal stability of polypropylene/montmorillonite nanocomposites. *Polymer Degradation and Stability, 82*(1), 127-131. https://doi.org/10.1016/S0141-3910(03)00173-3

14 Qin, H., Zhang, S., Zhao, C., Hu, G., & Yang, M. (2005). Flame retardant mechanism of polymer/clay nanocomposites based on polypropylene. *Polymer, 46*(19), 8386-8395. https://doi.org/10.1016/j.polymer.2005.07.019

15 Duvall, J., Sellitti, C., Myers, C., Hiltner, A., & Baer, E. (1994). Interfacial effects produced by crystallization of polypropylene with polypropylene-g-maleic anhydride compatibilizers. *Journal of applied polymer science, 52*(2), 207-216. https://doi.org/10.1002/app.1994.070520208

16 Lai, S. M., Chen, W. C., & Zhu, X. S. (2009). Melt mixed compatibilized polypropylene/clay nanocomposites: Part 1–The effect of compatibilizers on optical transmittance and mechanical properties. *Composites Part A: Applied Science and Manufacturing, 40*(6-7), 754-765. https://doi.org/10.1016/j.compositesa.2009.03.006

17 Lai, S. M., Chen, W. C., & Zhu, X. S. (2011). Melt mixed compatibilized polypropylene/clay nanocomposites. II. Dispersion vs. thermal properties, optical transmittance, and fracture behaviors. *Journal of composite materials, 45*(25), 2613-2631. https://doi.org/10.1016/j.compositesa.2009.03.006

18 Durmus, A., Woo, M., Kasgöz, A., Macosko, C. W., & Tsapatsis, M. (2007). Intercalated linear low density polyethylene (LLDPE)/clay nanocomposites prepared with oxidized polyethylene as a new type compatibilizer: structural, mechanical and barrier properties. *European Polymer Journal, 43*(9), 3737-3749. https://doi.org/10.1016/j.eurpolymj.2007.06.019

19 Bagheri-Kazemabad, S., Fox, D., Chen, Y., Geever, L. M., Khavandi, A., Bagheri, R., ... & Chen, B. (2012). Morphology, rheology and mechanical properties of polypropylene/ethylene–octene copolymer/clay nanocomposites: Effects of the compatibilizer. *Composites Science and Technology, 72*(14), 1697-1704. https://doi.org/10.1016/j.compscitech.2012.06.007

20 Reichert, P., Nitz, H., Klinke, S., Brandsch, R., Thomann, R., & Mülhaupt, R. (2000). Poly (propylene)/organoclay nanocomposite formation: Influence of compatibilizer functionality and organoclay modification. *Macromolecular Materials and Engineering, 275*(1), 8-17. https://doi.org/10.1002/(SICI)1439-2054(20000201)275:1%3C8::AID-MAME8%3E3.0.CO;2-6

21 Lee, S. S., & Kim, J. (2004). Surface modification of clay and its effect on the intercalation behavior of the polymer/clay nanocomposites. *Journal of Polymer Science Part B: Polymer Physics, 42*(12), 2367-2372. https://doi.org/10.1002/polb.20109

22 Dong, Y., & Bhattacharyya, D. (2010). Dual role of maleated polypropylene in processing and material characterisation of polypropylene/clay nanocomposites. *Materials Science and Engineering: A, 527*(6), 1617-1622. https://doi.org/10.1016/j.msea.2009.10.043

23 Ginzburg, V. V., Singh, C., & Balazs, A. C. (2000). Theoretical phase diagrams of polymer/clay composites: the role of grafted organic modifiers. *Macromolecules, 33*(3), 1089-1099. https://doi.org/10.1021/ma991324e

24 Balazs, A. C., Singh, C., & Zhulina, E. (1998). Modeling the interactions between polymers and clay surfaces through self-consistent field theory. *Macromolecules, 31*(23), 8370-8381. https://doi.org/10.1021/ma980727w

25 Gabr, M. H., Okumura, W., Ueda, H., Kuriyama, W., Uzawa, K., & Kimpara, I. (2015). Mechanical and thermal properties of carbon fiber/polypropylene composite filled with nano-clay. *Composites Part B: Engineering*, *69*, 94-100. https://doi.org/10.1016/j.compositesb.2014.09.033

26 Rao, G. R., Srikanth, I., & Reddy, K. L. (2021). Effect of organo-modified montmorillonite nanoclay on mechanical, thermal and ablation behavior of carbon fiber/phenolic resin composites. *Defence Technology*, *17*(3), 812-820. https://doi.org/10.1016/j.dt.2020.05.012

27 Fasihnia, S. H., Peighambardoust, S. H., & Peighambardoust, S. J. (2018). Nanocomposite films containing organoclay nanoparticles as an antimicrobial (active) packaging for potential food application. *Journal of Food Processing and Preservation*, *42*(2), e13488. https://doi.org/10.1111/jfpp.13488

28 Hong, C. H., Lee, Y. B., Bae, J. W., Jho, J. Y., Nam, B. U., & Hwang, T. W. (2005). Molecular weight effect of compatibilizer on mechanical properties in polypropylene/clay nanocomposites. *Journal of Industrial and Engineering Chemistry*, *11*(2), 293-296.

29 Chiu, F. C., Lai, S. M., Chen, J. W., & Chu, P. H. (2004). Combined effects of clay modifications and compatibilizers on the formation and physical properties of melt-mixed polypropylene/clay nanocomposites. *Journal of Polymer Science Part B: Polymer Physics*, *42*(22), 4139-4150. https://doi.org/10.1002/polb.20271

Қ.Н. Бердиназаров, Е.О. Хакбердиев, Н.Ф. Нормуродов Н.Р. Ашуров

Cloisite15A және Cloisite20A изотактикалық полипропилен композиттерінің механикалық және жылулық қасиеттері

Мақалада малеин ангидридімен (PP-g-MA) егілген полипропилен құрамының Cloisite15A және Cloisite20A интерстициалды кеңістіктегі модификатордың тығыздығымен ерекшеленетін саздың екі түрі бар полипропилен (PP) композицияларының термиялық және механикалық қасиеттеріне әсері зерттелген. PP/балшық композиттері 3, 6, 9 және 12 массалық % PP-g-MA әр түрлі құрамның қатысуымен балқытылған. Модификатордың жоғары тығыздығы бар Cloisite15A интеркалирленген құрылымдардың түзілуіне ықпал ететіні, ал модификаторы төмен Cloisite20A негізінен қабыршақтанған нанокомпозиттерді түзетіні анықталды. Бірінші жағдайда құрылым интеркалациялануға бейім, ал Cloisite20A композиттері негізінен қабыршақтанған құрылымдардың пайда болуын қолдайды. Нанокомпозиттің пайда болуы термиялық тұрақтылықтың айтарлықтай жоғарылауымен бірге жүреді (50% салмақ жоғалту полипропилен және оның негізіндегі нанокомпозиттер үшін сәйкесінше 360°C және 430°C температурада байқалады). Нанокомпозиттердің механикалық қасиеттерін талдау, жалпы алғанда, серпімділік модулінің 15–20%-ға артқанын көрсетеді (төмен модульді PPMA болуын ескере отырып) және бұл әсер қабыршақтанған құрылымдар үшін айқынырақ, кернеу кезінде аққыштық шегі іс жүзінде өзгермейді, ал сыну кезінде салыстырмалы ұзару айтарлықтай төмендейді.

Кілт сөздер: полипропилен, саз, композит, малеин ангидридті егілген полипропилен, интеркалация, қабыршақтану, тотығу, монтмориллонит.

К.Н. Бердиназаров, Э.О. Хакбердиев, Н.Ф. Нормуродов Н.Р. Ашуров

Механические и термические свойства изотактических полипропиленовых композитов с Cloisite15A и Cloisite20A

В статье изучено влияние содержания полипропилена, привитого малеиновым ангидридом (PP-g-MA), на термические и механические свойства композиций полипропилена (ПП) с двумя типами глин, различающихся плотностью модификатора в межслоевом пространстве, Cloisite15A и Cloisite20A. Композиты ПП/глина смешивались в расплаве в присутствии различного содержания PP-g-MA от 3, 6, 9 и 12 мас.%. Выявлено, что Cloisite15A с высокой плотностью модификатора способствует образованию интеркалированных структур, тогда как Cloisite20A с низкой плотностью модификатора формируют преимущественно эксфолированные нанокомпозиты. В первом случае структура имеет тенденцию к интеркалированию, в то время как композиты с Cloisite20A способствуют образованию преимущественно эксфолированных структур. Формирование нанокомпозита сопровождается значительным усилением термостабильности (50% потеря веса наблюдается при температурах 360 и 430ºC для полипропилена и нанокомпозитов на его основе, соответственно). Анализ механических свойств нанокомпозитов сведительствует, в целом, об увеличении модуля упругусти на 15–20 % (с учетом присутствия низкомодульного ППМА), причем этот эффект более выражен для эксфоилиированных структур, напряжение при пределе текучести практически не претерпевает изменений, а относительное удилинение при разрушении заметно уменьшается.

Ключевые слова: полипропилен, глина, композит, полипропилен с привитым малеиновым ангидридом, интеркаляция, эксфолиация, окисление, монтмориллонит.